

Amperimetric Biosensor Based on Carbon Nanotube and Plasma Polymer

Hitoshi Muguruma
Shibaura Institute of Technology
Japan

1. Introduction

Carbon nanotubes (CNTs) have been the focus of considerable studies since their discovery by Iijima (Iijima, 1991). CNTs are considered to be formed by the folding of graphene layers into carbon cylinders. They are of two distinct structural types: single-walled carbon nanotubes (SWCNTs) and multi-walled carbon nanotubes (MWCNTs). A SWCNT is a single shell extending from end to end with 1.3-2 nm tube diameter. A MWCNT is composed of several coaxial shells, each formed with rolled graphite sheets, with diameters varying from 2 to 50 nm and the distance between sheets being about 0.34 nm. CNTs have many new applications to electronic devices, such as field-effect transistors (Maki et al., 2006; Ohnaka et al., 2006) and gas sensors (Ueda et al., 2006; Wongwiriyan et al., 2005), because of their unique electronic properties, unique geometric structure, high mechanical strength, and high chemical stability.

Recently, amperometric biosensors using CNTs have been increasingly reported. The typical structure of a CNT-based amperometric biosensor is the combination of biomacromolecules (e.g., enzymes) and CNTs in the vicinity of the electrode. Because of the well-defined nanostructure of CNTs, a good connection between CNTs and enzymes can be obtained. CNTs also enhance the electron transfer from reaction center of enzyme to electrode. Therefore, high performance of biosensor characteristics can be realized. Many strategies has been reported: the treatment of CNTs with nitric or sulfonic acid in order to introduce the chemically active functional groups (Liu et al., 2005a; Gooding et al., 2003; Azamian et al., 2002; Kim et al., 2006; Li et al., 2005; Liu et al., 2006), which enables subsequent modification. Another strategy is the dispersion of CNTs with a binder such as Nafion (Tang et al., 2004; Tsai et al., 2005; Hrapovic et al., 2004; Lee et al., 2007), Teflon (Wang & Musameh, 2003), sol-gel (Gavalas et al., 2004; Salimi et al., 2004; Yang et al., 2006; Kandimalla et al., 2006), poly(methyl methacrylate) (PMMA) (Rege et al., 2003), redox hydrogel (Joshi et al., 2005; Wang et al., 2006), poly(dimethyldiallylammonium chloride) (Zhao & Ju, 2006; Yan et al., 2007), chitosan (Liu et al., 2005b; Rivas et al., 2007), and electropolymerized film (Tsai et al., 2006; Pan et al., 2005). However, these methods require that enzymes and other biomolecules receive careful treatment in order to retain their tertiary structure. Moreover, when using such wet processes, it is difficult to control the nanoscale fabrication. A method where the CNTs are directly treated by plasma has recently been reported (Khare et al., 2005; Khare et al., 2004; Khare et al., 2002; Plank et al., 2005). The

advantage of this modification is that chemically active functional groups, such as amino and carboxyl groups can be easily introduced on the side wall and/or edge of the CNTs without contamination. Also, our group proposed an amperometric biosensor based on a plasma polymer (Muguruma & Karube, 1999; Muguruma et al., 2000; Muguruma et al., 2005; Muguruma & Kase, 2006; Muguruma et al., 2006).

With this in mind, the combination of the PP and/or plasma modification has been explored with a CNT-based amperometric biosensor application. Here we choose a glucose oxidase as a model of enzyme family because of the most popular amperometric biosensor. The proposed strategy not only simplifies the configuration of the CNT-based biosensor composed of plasma polymer (PP) and the enzyme, but also provides high performance biosensor characteristics, such as high sensitivity, high selectivity toward targets, and reliability.

2. Plasma polymerization for biosensor design

In this section, the methods of preparation and the properties of plasma polymer are briefly described (Yasuda, 1985). The plasma polymer (PP) is achieved in a glow discharge or plasma in the vapor phase. The resulting polymer was directly deposited onto the substrate as a thin film. The typical apparatus for plasma polymerization is shown in Figure 1. The monomers are vaporized and filled into the chamber. Gas monomers and liquid monomers can be supplied by bombs and reservoirs, respectively. The starting monomer gases may not contain the type of functional groups (e.g. double bond) normally associated with conventional polymerization. The pressure and flow rate are appropriately controlled. The electromagnetic power is supplied to generate active species for polymerization and glow discharge occurs. Inductive coils or capacitance are used for the power supply and a radio frequency (RF) of 13.56 MHz is industrially available. The thin film is deposited onto the surface of substrate with a typical deposition rate of 10-100 nm/min. The parameters for polymerization are discharge power and frequency, monomer structure, reactor type, flow rate of monomer, plasma pressure, substrate temperature and substrate position (Yasuda, 1985). The properties of the film are attributed to the fact that the polymerization occurs with the participation of many active species in the plasma state. The structure of the ethylene plasma-polymerized films is, for example, different from that of polyethylene films. The latter consists of chains with a regular repeat unit whereas the former tends to form an irregular three-dimensional crosslinked network.

Introduction of surface amino groups with plasma polymer is a common step in biosensor fabrication processes. The surface amino group has dual characteristics; one is hydrophilicity, which allows for dense loading of biological components onto the film surface, and the other is its behavior as a seed for subsequent chemical grafting, such as changing the surface properties and covalent bond immobilization to prevent leaching of immobilized biomaterials. Allylamine is the most popular monomer for providing surface amino groups. Allylamine PP has been used as a porous membrane modification for reverse osmosis applications, due to the hydrophilic nature of the polymer backbone (Bell et al., 1975). Biomedical applications of allylamine PP were first reported by Muratsugu et al. (Muratsugu et al., 1991) in which the F(ab')₂ fragments of antibody proteins were densely immobilized on the surface of allylamine PP. Allylamine PPs were subsequently widely used in biomedical applications (Mahoney et al., 2004; Kurosawa et al., 2002; Basarir et al., 2007; Zhang et al., 2003; Zhang et al., 2005). The PP surfaces of ethylenediamine (EDA) and

alkylamines have amino groups and have also been used in biomedical applications (Jung et al., 2006; Nakanishi et al., 1996; Wang et al., 2003). The resulting film is sometimes different from that of the original monomer structure, because the plasma polymerization process involves fragmentation and reorganization in the presence of highly energetic active species. Therefore, plasma control during the production of biomedical PPs is the central issue; for example, the acetonitrile PP surface (Hiratsuka et al., 2000) and surfaces prepared by plasma treatment of nitrogen (Everhart & Reilley, 1981), ammonia (Hollahan et al., 1969), and a mixture of N_2/H_2 (Meyer-Plath et al., 2003) gas have amino groups, despite the original monomers having no amino groups. Chemical derivative X-ray electron spectroscopy (XPS) surface analysis and infrared (IR) spectroscopy of acetonitrile have shown that surface nitrogen is present not only as amino groups, but also as other nitrogen-based functional groups, such as C-NH-C, C-N=N-C, -C=N-, and -CN (Hiratsuka et al., 2000; Muguruma, 2008). The structure of the PP is characterized by highly branched and incompletely crosslinked aliphatic hydrocarbon backbone chains containing nitrogen atoms, and double bonds (C=C) are interspersed along the chains.

In summary, characteristics of PP include (i) easily control of the thickness range from several ten nanometer to micrometer, (ii) processing that facilitates the wetness and charge control of the surface properties, (iii) good adhesion to the substrate, (iv) ability to protect against interferant agents, and (v) an affinity with biological components. Therefore, PPs are suitable for the interfacial design between a biological component (enzyme) and an electrode.

3. Optimization for device fabrication

3.1 Device fabrication procedure

The preparation scheme is shown in Fig. 2. The device was formed on a 0.15-mm-thick glass substrate, with planar dimensions of approximately 50×50 mm². All the metal layers were sputter-deposited and patterned by a masking process. The glass slides used to make the thin film electrodes were boiled in a hydrogen peroxide/ammonia/water solution (approximately 1:1:8 by volume) for 1 h, and then rinsed with water and acetone. Au thin films were deposited using sputtering apparatus (VEP-1000, Ulvac Inc., Tokyo, Japan). A 40-nm-thick Cr intermediate layer was used to promote the adhesion of the Au layer. The dimension of the opening for the working electrode was 5×5 mm².

A plasma generator (VEP-1000, Ulvac Inc., Tokyo, Japan) was used to deposit a 6-nm-thick acetonitrile-PP (AN-PP) (first/lower PP) onto the sputtered Au electrode at 150 W and under a pressure of 0.6 Pa for a deposition time of 60 s. The CNTs were dispersed in a 1:1 mixed solution of ethanol and phosphate buffer solution (20 mM, pH 7.4) in which the optimized CNT concentration was 0.75 mg mL⁻¹. The CNT suspension was deposited dropwise onto the PP surface, and then dried in a vacuum oven. Subsequently, the CNT-adsorbed surface was treated with nitrogen plasma under the following parameters: power, 100 W (optimized); flow rate, 15 mL min⁻¹; pressure, 3 Pa; exposure time, 60 s. The enzyme was then added by dropping an aliquot of GOx (10 mg mL⁻¹) in phosphate buffer (20 mM, pH 7.4) onto the film. One hour later, the device was washed with water. Finally, the enzyme-adsorbed surface was overcoated with a second AN-PP (6 nm thickness), using the same deposition parameters as that for the first PP. The devices were stored in a refrigerator at 4 °C until use.

Cyclic voltammetry was performed using an electrochemical analyzer (Model 701A, ALS Instruments, West Lafayette, IN), with a three-electrode configuration. A reference electrode (Ag/AgCl, RE-1C) and a counter electrode (platinum wire) were purchased from Bioanalytical Systems Inc. Electrochemical measurements were carried out in a 10 mL vessel at ambient temperature (20 ± 1 °C). A phosphate buffer (20 mM, pH 7.4) was used as the supporting electrolyte. The measurement was carried out at least four times.

The fabricated amperometric biosensor based on CNT and PP has a unique sandwich-like structure of PP/GOx/CNT/PP/Au. The device was fabricated with a dry-chemistry basis of the layer-by-layer process. Figure 3 showed the SEM image of the device surface. In Fig 3a, the distinct CNT was not observed probably because surface concentration of CNT was small. Nevertheless, the large current response was obtained (discuss below). Therefore, the electrochemical contact is completed in this process. Fig. 3b supports the fact that the flat and homogeneous surface for enzyme immobilization is obtained. The each step of the fabrication processes was optimized.

3.2 Effectiveness of CNT

The effectiveness of using CNTs was examined and the results are given in Fig. 4. The amperometric response of the device with CNTs (PP/GOx/CNT/PP/Au, Fig. 4d) was 16-fold larger than that without CNTs (PP/GOx/PP/Au, Fig. 4a). The current response to the enzymatic reaction given by the CNT-PP electrode was the largest, and more than any other PP-based enzyme electrode, such as electron transfer mediators (Muguruma & Kase, 2006) and platinum electrodes (Muguruma et al., 2000). The obtained maximum current density of ca. 0.4 mA cm^{-2} was comparable with that of other CNT-based biosensors (Tang et al., 2004; Joshi et al., 2005; Pan et al., 2005; Patolsky et al., 2004).

Two mechanisms can be considered for the large current response; the direct electron transfer via the CNTs, and the catalytic ability of the CNTs (Merkoçi et al, 2005; Wang and Musameh, 2003; Salimi et al, 2004; Liu et al., 2005) toward hydrogen peroxide generated by the enzymatic reaction. The latter is supported by the fact that oxidation currents with CNT-based electrodes start at around +0.2 V. The electrode with sputtered platinum (Pt), which also has catalytic ability (PP/GOx/PP/Pt, Fig. 4b), displays an oxidation peak at $>+0.2$ V. The current at $>+0.6$ V for PP/GOx/CNT/PP/Au (Fig. 4d) was much larger than that for PP/GOx/PP/Pt, which suggests that the CNTs provide enhancement of electron transfer as an electron conductive component of the electrode. (a) The manuscript must be written in English, (b) use common technical terms, (c) avoid abbreviations, don't try to create new English words, (d) spelling: Follow Merriam Webster's Collegiate Dictionary, Longman or Oxford Dictionaries.

3.3 Effectiveness of the first PP layer between the Au electrode and CNTs

The current observed for the electrode with the first PP layer (PP/GOx/CNT/PP/Au, Fig. 4d) after glucose addition was much larger than that for the electrode without the PP layer (PP/GOx/CNT/Au, Fig. 4c), which indicates that the first PP layer acts as an interface between the Au electrode and the GOx-CNT complex. In fact, a densely packed array of GOx molecules can be formed on the hydrophilic and positively charged surface of acetonitrile PP than on a bare Au electrode. Because the enzyme layer on the PP surface is two dimensional, this process does not depend on the thickness or the loading amount of the enzyme (Muguruma et al., 2000; Muguruma et al., 2006).

The background current of the electrode with the first PP layer (Fig. 4c) was smaller than that for the device without the PP layer (Fig. 4d). Two reasons are considered for this. One reason is that the nano-sandwich structure does not enlarge the effective geometric area (i.e. very flat surface) of the electrode, and the other is that the PP layer appears to present a diffusion barrier to the supporting electrolyte, causing a partitioning between the electrode and the bulk solution (Muguruma et al., 2000).

From atomic force microscopic measurements of the surface, the dimension of a GOx molecule is observed as a compact ellipsoid with an approximate dimension of $12.2 \times 8.3 \text{ nm}^2$ (Muguruma et al., 2006). One dimension of a single-walled CNT (1.2-2.0 nm) is smaller than that of a GOx molecule; therefore, an effective electrochemical contact of the GOx-CNT-Au electrode can be achieved.

3.4 Optimization for GOx-CNT mixture

Since the CNTs are chemically inert and insoluble in most solvents, solution casting of the CNT layer was achieved by temporal dispersion of the CNTs in solution. The cyclic voltammetry (CV) response of the PP/GOx/PP/Au biosensor with a CNT layer cast using a 1:1 mixture of buffer and ethanol displayed a response higher than that of CNT layers cast using only buffer or only ethanol, as shown in Fig. 5. This confirms that the 1:1 buffer/ethanol mixture provides a more stable CNT suspension, as shown by the photograph of vial suspensions in Fig. 5. However, this suspension is less stable than that obtained by other processes using binder such as Nafion, polypyrrole, and surfactants (Hrapovic et al., 2004; Joshi et al., 2005; Wang et al., 2006; Gavalas et al., 2004; Merkoçi et al., 2005). Therefore, it is probable that the CNT layer is mechanically and electrically loose (probably slack packing). Combined with the subsequent plasma treatment, a high sensor response was obtained (Fig. 5c). This method for the formation and modification of a CNT layer is a very simple and clean process.

3.5 Optimization of CNT concentration in solution for CNT layer casting formation

Optimization of the CNT concentration in the suspension solution for casting was carried out. Figure 6 shows CVs obtained in the presence and absence of glucose as a function of the CNT concentration. Comparing Figs. 6a and 6b, it can be seen that the current due to glucose addition to the device with CNTs at 0.75 mg mL^{-1} was larger than that with 0.3 mg mL^{-1} . From the CV with the largest concentration of 15 mg mL^{-1} (Fig. 6), both the oxidation and background currents increased. The CNT acts as the catalyst or direct electron transfer via CNT (discussed next section). From these mechanisms, in spite of higher concentration of CNT, the output current in higher CNT concentration of 15 mg/mL decreased than that of 0.75 mg mL^{-1} . This is because the amount of CNT is so large compared with enzyme GOx that generation of hydrogen peroxide and electron due the enzymatic reaction toward glucose reduced. This shows that the design for enzyme-CNT electrode need to consider the balance between the amount of enzyme and CNT. Therefore, the optimized concentration of CNTs was determined as 0.75 mg mL^{-1} , due to the largest increment in current with glucose addition.

3.6 Optimization of plasma power for treatment of CNT layer

A subsequent CNT modification on the first PP layer is a key step. The CNT is directly treated by oxygen or nitrogen plasma instead of a wet-chemical treatment for CNTs. The

effectiveness of plasma treatment on the CNT was investigated. The fabricated amperometric biosensor has a unique sandwich-like structure denoted as the basic structure of PP/GOD/PT/CNT/PP/Au. Figure 8 show cyclic voltammograms obtained in the absence and presence of glucose. First, the effectiveness of CNTs and oxygen plasma treatment (PT) for CNTs was investigated. The current responses of the devices without CNTs (PP/GOx/PP/Au, Fig. 8a) and oxygen plasma treatment (PP/GOx/CNT/PP/Au, Fig. 7b) were much smaller than that of the optimized device (PP/GOx/PT-70W/CNT/PP/Au, Fig. 7f). The higher the power of oxygen plasma for modifying CNTs, the larger the increase in current for sensor response. In PP/GOx/PT-60W/SWCNT/PP/Au (Fig. 7e) and PP/GOx/PT-70W/SWCNT/PP/Au (Fig. 7f), upon the addition of glucose, the observed current changed markedly with a large increase in oxidation current. Additionally, we confirmed that the current observed for the electrode with the first PP layer (PP/GOx/PT/CNT/PP/Au) after glucose addition was 4-5-fold larger than that for the electrode without the PP layer (PP/GOx/PT/CNT/Au), which indicates that the first PP layer acts as an interface between the Au electrode and the GOx-CNT complex.

Figure 8 summarizes the current of the PP/GOx/CNT/PP/Au device as a function of plasma power for the treatment of CNTs on the first PP layer (CV data were shown in Fig. 7). It was concluded that the optimal plasma power for CNT-treatment was 70-100 W. The oxidation current response to 48 mM glucose initially increases, plateaus, and then decreases with increasing plasma power treatment of the CNTs. At less than 70 W, the CNT modification is insufficient for suitable contact with the GOx. At more than 150 W, the current decreases, because the higher energy of the plasma species has etched the mechanical structure of CNTs and a detrimental effect on the electronic properties of the CNTs. However, the electronic properties of CNTs were almost retained less than 100-W of the plasma power because the large current sensor response was comparable with the other CNT-base biosensor (Azaman et al., 2002; Hrapovic et al., 2004; Tsai et al., 2005).

These results indicate that both PP and nitrogen (or oxygen) plasma modification is an effective strategy for fabrication of an enzyme-friendly platform in CNT-based amperometric biosensors. The effectiveness of the nitrogen or oxygen plasma treatment is probably due to the introduction of carboxyl or amino groups to the side wall surface of the CNTs. This experimental evidence of introduction of functional groups is experimentally reported by Khare's group (Khare et al., 2005; Khare et al., 2004; Khare et al., 2002).

As a result, the hydrophobic surface of the CNTs is changed to a stable hydrophilic environment that facilitates contact with GOx. Additionally, when comparing between nitrogen and oxygen plasma treatment, the current response with nitrogen plasma was slightly larger than that with oxygen plasma. This is attributed to difference of functional groups. Nitrogen plasma treatment can introduce positive charge (amino) groups, whereas oxygen plasma treatment can introduce negative charge (carboxyl) groups (Everhart and Reilly, 1981). Therefore, the negatively charged GOx ($pI = 4.2$) is densely loaded onto positively charged surfaces than onto negatively charged surfaces (Muguruma et al., 2006).

3.7 Comparison between single- and multi-walled CNT

Figure 9 shows the responses of several glucose sensors, each of which was prepared using different types of CNT: single-walled CNT and multi-walled CNT (SWCNTs, 20-30-nm-diameter MWCNTs, and 40-70-nm-diameter MWCNTs). When comparing these CNTs, the increment in current is SWCNTs > 20-30-nm-diameter MWCNTs > 40-70-nm-diameter MWCNTs. SWCNTs are the most suitable materials among CNTs. However, the

relationship between current due to glucose and plasma power for the treatment of MWCNT is unclear. The possible explanation for this is that the GOx molecule is a compact ellipsoid with approximate dimensions of 12.2×8.3 nm² (measured by atomic force microscopy) (Muguruma et al., 2005). Then, the redox center exists at the smaller pocket in the larger (10 nm) three-dimensional structure of GOx. The dimension of SWCNTs (1.2-2 nm) is smaller than that of GOx, whereas that of MWCNTs (> 20 nm) is larger than that of GOx. Therefore, almost all of the reaction centers of GOx were intact and connected to SWCNTs.

3.8 Effectiveness of the second PP layer over the immobilized enzyme

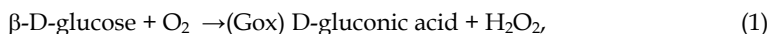
The final step was the overcoating of acetonitrile PP (denoted as the second PP layer) onto the immobilized GOx and CNTs. Our group has already reported that the GOx adsorbed on the surface was more deeply embedded, immobilized within the second acetonitrile PP layer (Muguruma & Kase, 2006). Two thicknesses were investigated for the second PP coating; 10 nm and 20 nm. The 10-nm-thick PP layer probably provides a coating to completely cover the adsorbed enzyme because the height of the GOx monolayer was 6-7 nm (Muguruma & Kase, 2006). In spite of the fact that GOx was treated by high-energy plasma, the response to 2.5 mM glucose with the second PP coating film is almost the same as that with no second PP layer on the device; that is, the initial enzymatic activity of GOx is retained. This means that under milder exposure to organic plasma, the enzyme does not become seriously dysfunctional, as previously demonstrated (Muguruma et al., 2005; Muguruma and Kase, 2006). The fact that the glucose response of the devices with and without the second PP layer were similar shows that the coating is not a barrier toward access by glucose.

Figure 10 shows a comparison of the amperometric response due to an interferant (ascorbic acid) and glucose. The maximum level of ascorbic acid under physiological conditions is 0.5 mM. From our previous report, the first acetonitrile PP layer reduces the effect of interference. This was attributed to the first PP layer serving a role as an anti-fouling coating against oxidizing interference (Muguruma et al., 2000). The first PP layer can incompletely eliminate the current due to interference. In fact, the device without a second acetonitrile PP layer (GOx/CNT/PP/Au) shows a current of 2 μ A due to 0.5 mM ascorbic acid in which this is similar with the current due to the response of 0.14 mM glucose (Fig. 10a). If the coating film is thicker, then the oxidation current due to ascorbic acid is smaller. The effect of addition of ascorbic acid to the response of the device with a 20-nm-thick PP coating (PP/GOx/CNT/PP/Au) was negligible (almost similar with background, Fig. 10c), because the access of ascorbic acid to the CNTs is blocked by the second PP coating. Therefore, the second PP layer completely eliminates interference and enables the selective detection of glucose.

The other advantage of the second PP layer is also demonstrated in Fig.11. The operational stability under continuous polarization at +0.8 V in the presence of 48 mM glucose was investigated. For the device without the second PP coating, the current decreased to 25% of the initial current after 24 h, due to leaching of the physically adsorbed GOx and CNTs onto the first PP layer. In contrast, the electrochemical response of the device with the second PP layer retained a current response of more than 90%. This suggests that the overcoating with a second acetonitrile PP layer prevents leaching and contamination of the GOx and CNTs.

3.9 Mechanism of sensor response

Two mechanisms can be considered for the large current response. One is the catalytic activity of the CNTs (Kim et al., 2006; Tang et al., 2004; Hrapovic et al., 2004) toward hydrogen peroxide generated by the enzymatic reaction. GOx specifically catalyzes the oxidation of glucose as follows:

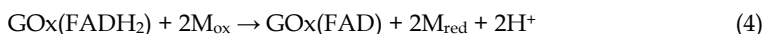


and the CNT catalyzes the reaction of hydrogen peroxide as follows:



The Au electrode receives the electron, and as a result, the current increases.

The other mechanism is the direct electron transfer via the CNTs, and a possible mechanism is



where FAD locates in the vicinity of the reaction center of GOx, and M represents an electron transfer mediator.

4. Sensor performance

The previous sections have presented the optimization of the sensor fabrication process based on CNTs and PP. Here, the sensor performance of the optimized device is demonstrated. In Fig. 12, a steady state amperometric response at +0.8 V vs. Ag/AgCl was demonstrated for a wide range of glucose concentration (0.025-14 mM). The remarkable characteristic is the small background current ($0.35 \pm 0.013 \mu\text{A}$) compared with the glucose response, indicating there is no need to calibrate the baseline for the glucose measurement. This is because the nano-sandwich structure and the permselective coating of the first PP layer on the Au electrode provide effective electrochemical communication.

The nanometer size sandwich-like configuration provides a suitable distance for electrochemical communication between the electrode and the reaction center of the enzyme. As a result, a short response time (<4 s, 95% to maximum response) was obtained. The detection limit (signal/noise ratio: 3) of 6 μM is much lower than that of GOx/PP/Pt electrode (0.25 mM) (Muguruma et al., 2000). Since the devices were fabricated in the same batch, reasonable reproducibility (relative standard deviation: 3%, $n=4$) from sample-to-sample was obtained.

Figure 13 show the current vs. glucose concentration based on the data from Fig. 12. The characteristics of this device display good linearity ($r=0.993$) in the low concentration region (0.025-2.2 mM) and the sensitivity was 42 $\mu\text{A mM}^{-1} \text{cm}^{-2}$. Deviation from linearity is observed at higher (>5 mM) glucose concentration, representing a typical characteristic of the Michaelis-Menten model. The apparent Michaelis-Menten activity (K_M^{app}) of the immobilized enzyme was calculated according to the Lineweaver-Burk plot shown in the upper inset of Fig. 13. According to this, the K_M^{app} is calculated to be 11 mM. This value is similar to that of other CNT-based glucose biosensor (Tang et al., 2004; Liu et al., 2005) and is smaller than that of GOx in solution (33 mM) (Liu et al., 2005).

5. Conclusion

A new simple and reliable method for the fabrication of a CNT-based amperometric biosensor was demonstrated. CNTs and GOx enzyme were sandwiched between 6-nm-thick PPs on a sputtered gold electrode. Optimization of the casting formation of a CNT layer onto the lower PP was stressed. An organic plasma polymer coating method and a semiconductor-technology-compatible layer-by-layer process provided a well-defined nanocomposite of enzyme, CNTs, and PPs. This highly efficient electron transfer system was able to detect a relevant bioelectrochemical signal equal to 0.44 mA cm^{-2} . This also suggests that the PP and/or plasma process is a suitable interface design for electrochemical communication from the reaction center of GOx to an electrode via CNTs. The method presented here can be easily extended to other biosensor devices using other enzymes and proteins. As a simple dry process intended for mass production, this might be of benefit to the development of microscale and/or arrayed sensors.

6. References

- Azamian, B.R.; Davis, J.J.; Colemann, K.S.; Bagshaw, C.B. & Green, M.L.H. (2002). Bioelectrochemical single-walled carbon nanotubes, *J. Am. Chem. Soc.*, 124., 12664-12665.
- Basarir, F.; Cuong, N.; Song, W.-K. & Yoon, T.-H. (2007). Surface modification via plasma polymerization of allylamine for antibody immobilization, *Macromol. Symp.*, 249-250., 61-66.
- Bell, A.T.; Wydeven, T. & Johnson, C.C. (1975). A study of the performance and chemical characteristics of composite reverse osmosis membranes prepared by plasma polymerization of allylamine, *J. Appl. Polym. Sci.*, 19., 1911-1930.
- Cai, C. & Chen, J. (2004). Direct electron transfer of glucose oxidase promoted by carbon nanotubes, *Anal. Biochem.*, 332., 75-83.
- Everhart, D.S. & Reilley, C.N. (1981). Chemical derivatization in electron spectroscopy for chemical analysis of surface functional group introduced on low-density polyethylene film, *Anal. Chem.*, 53., 665-676.
- Gavalas, V.G.; Law, S.A.; Ball, J.C.; Andrews, R. & Bachas, L.G. (2004). Carbon nanotube aqueous sol-gel composites: enzyme-friendly platforms for the development of stable biosensors, *Anal. Biochem.*, 329., 247-252.
- Gooding, J.J.; Wibowo, R.; Liu, J.; Yang, W.; Losic, D.; Orbons, S.; Mearns, F.J.; Shapter, J.G. & Hibbert, D.B. (2003). Protein electrochemistry using aligned carbon nanotube arrays, *J. Am. Chem. Soc.*, 125., 9006-9007.
- Guldi, D.M.; Rahman, G.M.A.; Zerbetto, F. & Prato, M. (2005). Carbon Nanotubes in Electron Donor-Acceptor Nanocomposites, *Acc. Chem. Res.*, 38., 871-878.
- Hiratsuka, A.; Muguruma, H.; Nagata, R.; Nakamura, R.; Sato, K.; Uchiyama, S. & Karube, I. (2000). Mass transport behavior of electrochemical species through plasma-polymerized thin film on platinum electrode, *J. Membr. Sci.*, 175., 25-34.
- Hollahan, J.R.; Stafford, B.B.; Falb, R.D. & Payne, S.T. (1969). Attachment of amino group to polymer surface by radiofrequency plasmas, *J. Appl. Polym. Sci.*, 13., 807-816.
- Hrapovic, S.; Liu, Y.; Male, K.B. & Luong, J.H.T. (2004). Electrochemical biosensing platforms using platinum nanoparticles and carbon nanotubes, *Anal. Chem.*, 76., 1083-1088.

- Iijima, S. (1991). Helical microtubules of graphitic carbon, *Nature*, 354., 56-58.
- Joshi, P.P.; Merchant, S.A.; Wang, Y. & Schmidtke, D.W. (2005). Amperometric biosensors based on redox polymer-carbon nanotube-enzyme composites, *Anal. Chem.*, 77., 3183-3188.
- Jung, D.; Yeo, S.; Kim, J.; Kim, B.; Jin, B. & Ryu, D. Formation of amine groups by plasma enhanced chemical vapor deposition and its application to DNA array technology, *Surf. Coatings Tech.*, 200., 2886-2891.
- Kandimalla, V.B.; Tripathi, V.S. & Ju, H. (2006). A conductive ormosil encapsulated with ferrocene conjugate and multiwall carbon nanotubes for biosensing application, *Biomaterials*, 27., 1167-1174.
- Khare, B.; Wilhite, P.; Tran, B.; Teixeira, E.; Fresquez, K.; Mvondo, D.N.; Bauschlicher, Jr., C. & Meyyappam, M. (2005). Functionalization of carbon nanotubes via nitrogen glow discharge, *J. Phys. Chem. B*, 109., 23466-23472.
- Khare, B.; Wilhite, P.; Quinn, R.C.; Chen, B.; Schingler, R.H.; Tran, B.; Imanaka, H.; So, C.R.; Bauschlicher, Jr., C. & Meyyappam, M. (2004). Functionalization of carbon nanotubes by ammonia glow-discharge: experiments and modeling, *J. Phys. Chem. B*, 108., 8166-8172.
- Khare, B.; Meyyappam, M.; Cassell, A.M.; Nguyen, C.V. & Han, J. (2002). Functionalization of carbon nanotubes using atomic hydrogen from a glow discharge, *Nano Lett.*, 2., 73-77.
- Kim, J.-Y.; Baek, J.Y.; Kim, H.H.; Lee, K.A. & Lee, S.H. (2006) Integration of enzyme immobilized single-walled carbon nanotubes mass into the microfluidic platform and its application for the glucose-detection, *Sens. Actuators A*, 128., 7-13.
- Kurosawa, S.; Hirokawa, T.; Kashima, K.; Aizawa, H.; Park, J.-W.; Tozuka, M.; Yoshimi, Y. & Hirano, K. (2002). Adsorption of anti-C-reactive protein monoclonal antibody and its F(ab')₂ fragment on Plasma-Polymerized Styrene, allylamine and acrylic acid coated with quartz crystal microbalance, *J. Photopolym. Sci. Tech.*, 15., 328-330.
- Lee, C.-H.; Wang, S.-C.; Yuan, C.-J.; Wen, M.-F. & Chang, K.-S. (2007). Comparison of amperometric biosensors fabricated by palladium sputtering, palladium electrodeposition and Nafion/carbon nanotube casting on screen-printed carbon electrodes, *Biosen. Bioelectron.*, 22., 877-884.
- Li, J.; Wang, Y.-B.; Qiu, J.-D.; Sun, D.-C. & Xia, X.-H. (2005). Biocomposites of covalently linked glucose oxidase on carbon nanotubes for glucose biosensor, *Anal. Bioanal. Chem.*, 383., 918-922.
- Liu, G. & Lin, Y. (2006). Amperometric glucose biosensor based on self-assembling glucose oxidase on carbon nanotubes, *Electrochem. Commun.*, 8., 251-256.
- Liu, J.; Chou, A.; Rahmat, W.; Paddon-Row, M.N. & Gooding, J.J. (2005a). Achieving direct electrical connection to glucose oxidase using aligned single walled carbon nanotube arrays, *Electroanalysis*, 17., 38-46.
- Liu, Y.; Wang, M.; Zhao, F.; Xu, Z. & Dong, S. (2005b). The direct electron transfer of glucose oxidase and glucose biosensor based on carbon nanotubes/chitosan matrix, *Biosen. Bioelectron.*, 21., 984-988.
- Mahoney, D.J.; Whittle, J.D.; Milner, C.M.; Clark, S.J.; Mulloy, B.; Buttle, D.J.; Jones, G.C.; Day, A.J. & Short, R.D. (2004). A method for the non-covalent immobilization of heparin to surfaces, *Anal. Biochem.*, 330., 123-129.

- Maki, H.; Sato, T. & Ishibashi, K. (2006). Transport characteristic control of field-effect transistors with single-walled carbon nanotube films using electrode metals with low and high work functions, *Jpn. J. Appl. Phys.*, 45, 7234-7236.
- Merkoçi, A.; Pumera, M.; Llopis, X.; Pérez, B.; Valle, M. & Alegret, S. (2005). New materials for electrochemical sensing vi: carbon nanotubes, *Trend. Anal. Chem.*, 24., 826-838.
- Meyer-Plath, A.A.; Schröder, K.; Finke, B. & Ohl, A. (2003). Current trends in biomaterial surface functionalization–nitrogen-containing plasma assisted processes with enhanced selectivity, *Vacuum*, 71., 391-406.
- Muguruma, H.; Hiratsuka, A. & Karube, I. (2000). Thin film glucose biosensor based on plasma-polymerized film: simple design for mass production, *Anal. Chem.*, 72., 2671-2675.
- Muguruma, H. & Karube, I. (1999). Plasma-polymerized films for Biosensors, *Trend. Anal. Chem.*, 18., 62-68.
- Muguruma, H.; Kase, Y. & Uehara, H. (2005). Nanothin ferrocene film plasma polymerized over physisorbed glucose oxidase: toward high throughput fabrication of bioelectronic devices without chemical modifications, *Anal. Chem.*, 77., 6557-6562.
- Muguruma, H. & Kase, Y. (2006). Structure and biosensor characteristics of complex between glucose oxidase and plasma-polymerized nanothin film, *Biosens. Bioelectron.*, 22., 737-743.
- Muguruma, H.; Kase, Y.; Murata, N. & Matsumura, K. (2006). Adsorption of glucose oxidase onto plasma-polymerized film characterized by atomic force microscopy, quartz crystal microbalance, and electrochemical measurement, *J. Phys. Chem. B*, 110., 26033-26039.
- Muguruma, H. (2008). Quantitative characterization of surface amino groups of plasma-polymerized films prepared from nitrogen-containing monomers for bioelectronic applications, *IEICE Trans. Electron.*, E91-C., 963-967.
- Muratsugu, M.; Kurosawa, S. & Kamo, N. (1991). Adsorption and desorption of F(ab')₂ anti-hIgG on plasma-polymerized allylamine thin film: the application of the film to immunoassay, *J. Colloid Interf. Sci.*, 147, 378-386.
- Nakanishi, K.; Muguruma, H. & Karube, I. (1996). A novel method of immobilizing antibodies on a quartz crystal microbalance using plasma-polymerized films for immunosensors, *Anal. Chem.*, 68., 1695-1700.
- Ohnaka, H.; Kojima, Y.; Kishimoto, S.; Ohno, Y. & Mizutani, T. (2006). Fabrication of carbon nanotube field effect transistors using plasma-enhanced chemical vapor deposition grown nanotubes, *Jpn. J. Appl. Phys.*, 45., 5485-5489.
- Pan, D.; Chen, J.; Yao, S.; Tao, W. & Nie, L. (2005). An amperometric glucose biosensor based on glucose oxidase immobilized in electropolymerized poly(*o*-aminophenol) and carbon nanotube composite film on a gold electrode, *Anal. Sci.*, 21., 367-371.
- Patolsky, F.; Weizmann, Y. & Willner, I. (2004). Long-range electrical contacting of redox enzyme by SWCNT connectors, *Angew. Chem. Int. Ed.*, 43., 2113-2117.
- Plank, N.O.V.; Forrest, G.A.; Cheung, R. & Alexander, A.J. (2005). Electronic properties of n-type carbon nanotubes prepared by CF₄ plasma fluorination and amino functionalization, *J. Phys. Chem. B*, 109., 22096-22101.
- Rege, K.; Raravikar, N.R.; Kim, D.-Y.; Schadler, L.S.; Ajayan, P.M. & Dordick, J.S. (2003). Enzyme-polymer-single walled carbon nanotube composites as biocatalytic films, *Nano Lett.*, 3., 829-832.

- Rivas, G.A.; Miscoria, S.A.; Desbrieres, J. & Barrera, G.D. (2007). New biosensing platforms based on the layer-by-layer self-assembly of polyelectrolytes on Nafion/carbon nanotubes-coated glassy carbon electrodes, *Talanta*, 71., 270-275.
- Salimi, A.; Compton, R.G. & Hallaj, R. (2004). Glucose biosensor prepared by glucose oxidase encapsulated sol-gel and carbon-nanotube-modified basal plane pyrolytic graphite electrode, *Anal. Biochem.*, 333., 49-56.
- Tasis, D.; Tagmatarchis, N.; Bianco, A. & Prato, M. (2006). Chemistry of carbon nanotubes, *Chem. Rev.*, 106., 1105-1136.
- Tang, H.; Chen, J.; Yao, S.; Nie, L.; Deng, G. & Kuang, Y. (2004). Amperometric glucose biosensor based on adsorption of glucose oxidase at platinum nanoparticle-modified carbon nanotube electrode, *Anal. Biochem.*, 331., 89-97.
- Tsai, Y.-C.; Li, S.-C. & Liao, S.-W. (2006). Electrodeposition of polypyrrole-multiwalled carbon nanotube-glucose oxidase nanobiocomposite film for the detection of glucose, *Biosen. Bioelectron.*, 22., 495-500.
- Tsai, Y.-C., Li, S.-C. & Chen, J.-M. (2005). Cast thin film biosensor design based on a Nafion backbone, a multiwalled carbon nanotube conduit, and a glucose oxidase function, *Langmuir*, 21., 3653-3658.
- Ueda, T.; Norimatsu, H.; Hossain Bhuiyan, Md.M.; Ikegami, T. & Ebihara, K. (2006). NO sensing property of carbon nanotube based thin film gas sensors prepared by chemical vapor deposition techniques, *Jpn. J. Appl. Phys.*, 45., 8393-8397.
- Wang, H.; Wang, C.; Lei, C.; Wu, Z.; Shen, G. & Yu, R. (2003). A novel biosensing interfacial design produced by assembling nano-Au particles on amine-terminated plasma-polymerized films, *Anal. Bioanal. Chem.*, 377., 632-638.
- Wang, J. & Musameh, M. (2003). Carbon nanotube/Teflon composite electrochemical sensors and biosensors, *Anal. Chem.*, 75., 2075-2079.
- Wang, J.; Musameh, M. & Lin, Y. (2003). Solubilization of carbon nanotubes by Nafion toward the preparation of amperometric biosensors, *J. Am. Chem. Soc.*, 125., 2408-2409.
- Wang, Y.; Joshi, P.P.; Hobbs, K.L.; Johnson, M.B. & Schmidtke, D.W. (2006). Nanostructured biosensors built by layer-by-layer electrostatic assembly of enzyme-coated single-walled carbon nanotubes and redox polymers, *Langmuir*, 22., 9776-9783.
- Wongwiriyan, W.; Honda, S.; Konishi, H.; Mizuta, T.; Ikuno, T.; Ito, T.; Maekawa, T.; Suzuki, K.; Ishikawa, H.; Oura, K. & Katayama, M. (2005). Single-walled carbon nanotube thin-film sensor for ultrasensitive gas detection, *Jpn. J. Appl. Phys.*, 44., L482-L484.
- Yan, X.B.; Chen, X.J.; Tay, B.K. & Khor, K.A. (2007). Transparent and flexible glucose biosensor via layer-by-layer assembly of multi-wall carbon nanotubes and glucose oxidase, *Electrochem. Commun.*, 9., 1269-1275.
- Yang, M.; Yang, Y.; Liu, Y.; Shen, G. & Yu, R. (2006). Platinum nanoparticles-doped sol-gel/carbon nanotubes composite electrochemical sensors and biosensors, *Biosen. Bioelectron.*, 21., 1125-1131.
- Yasuda, H. (1985). *Plasma Polymerization*, Academic Press, Inc. ISBN 0-12-768760-2, Orland, Florida.
- Zhang, Z.; Chen, Q.; Knoll, W.; Foerch, R.; Holcomb, R. & Roitman, D. (2003). Plasma polymer film structure and DNA probe immobilization, *Macromolecules*, 36., 7689-7694.

Zhang, Z.; Knoll, W.; Foerch, R.; Holcomb, R. & Roitman, D. (2005). DNA hybridization on plasma-polymerized allylamine, *Macromolecules*, 38., 1271-1276.

Zhao, H. & Ju, H. (2006). Multilayer membranes for glucose biosensing via layer-by-layer assembly of multiwall carbon nanotubes and glucose oxidase, *Anal. Biochem.*, 350., 138-144.

7. Figures

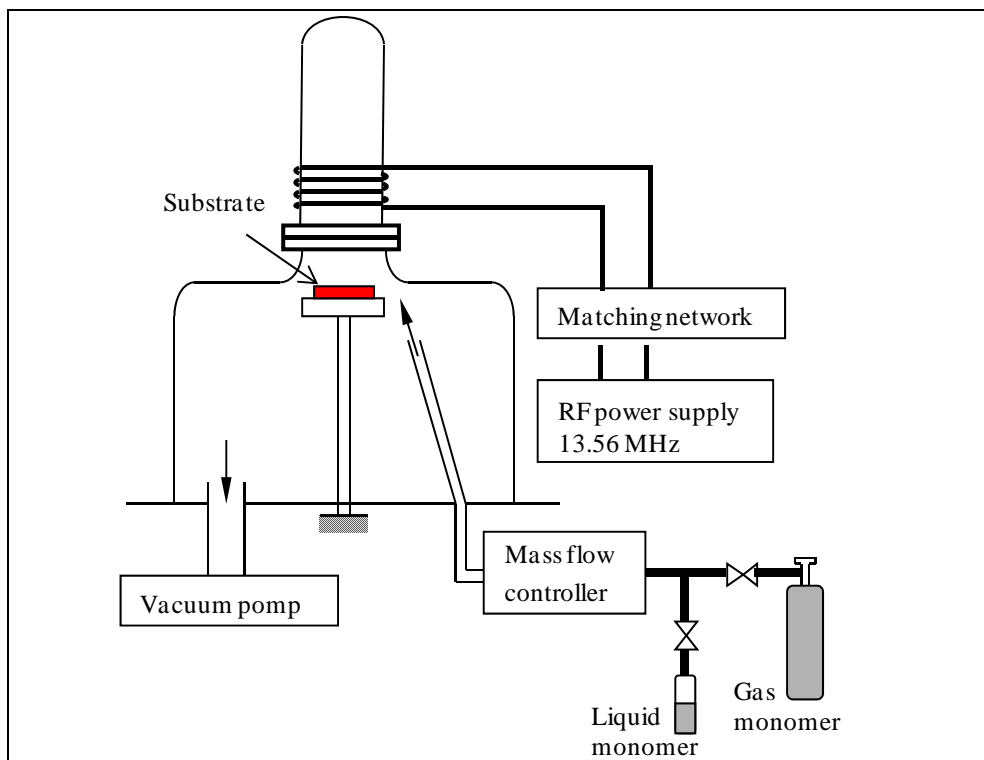


Fig. 1. Schematic representation of typical apparatus for plasma polymer.

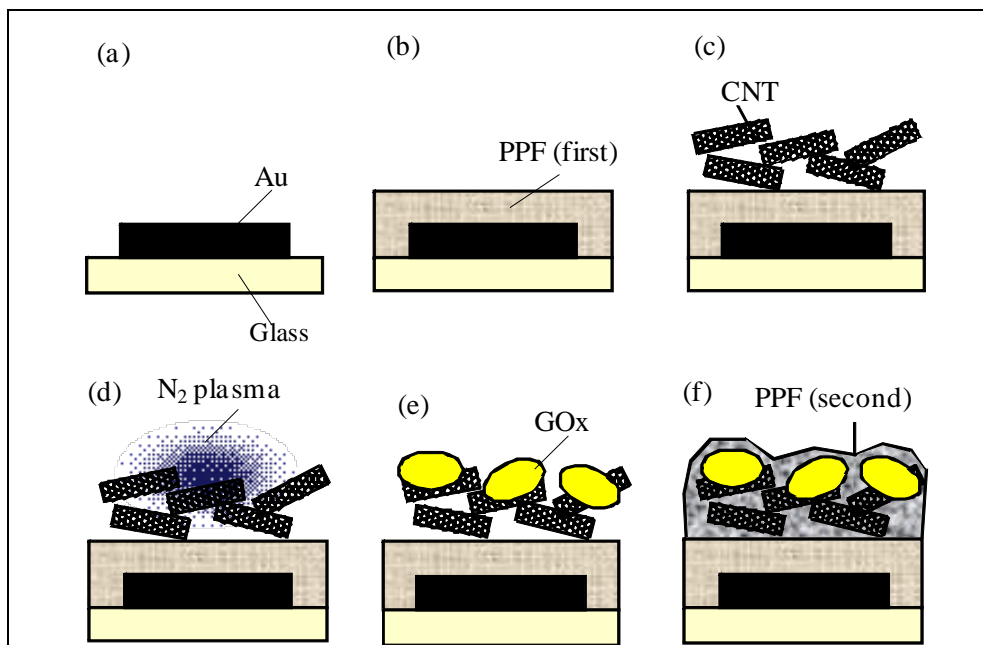


Fig. 2. Schematic representation of the fabrication of an amperometric biosensor based on CNT and PPs. (a) Au electrodes are sputtered onto a glass substrate through a metal mask. (b) A 6-nm-thick acetonitrile plasma-polymerized film (first PP) was deposited. (c) Solution casting is used to form the CNT layer. (d) Nitrogen plasma treatment of the CNT layer. (e) Solution casting of the enzyme layer onto the CNT layer. (f) Immobilized GOx is overcoated by a second PP.

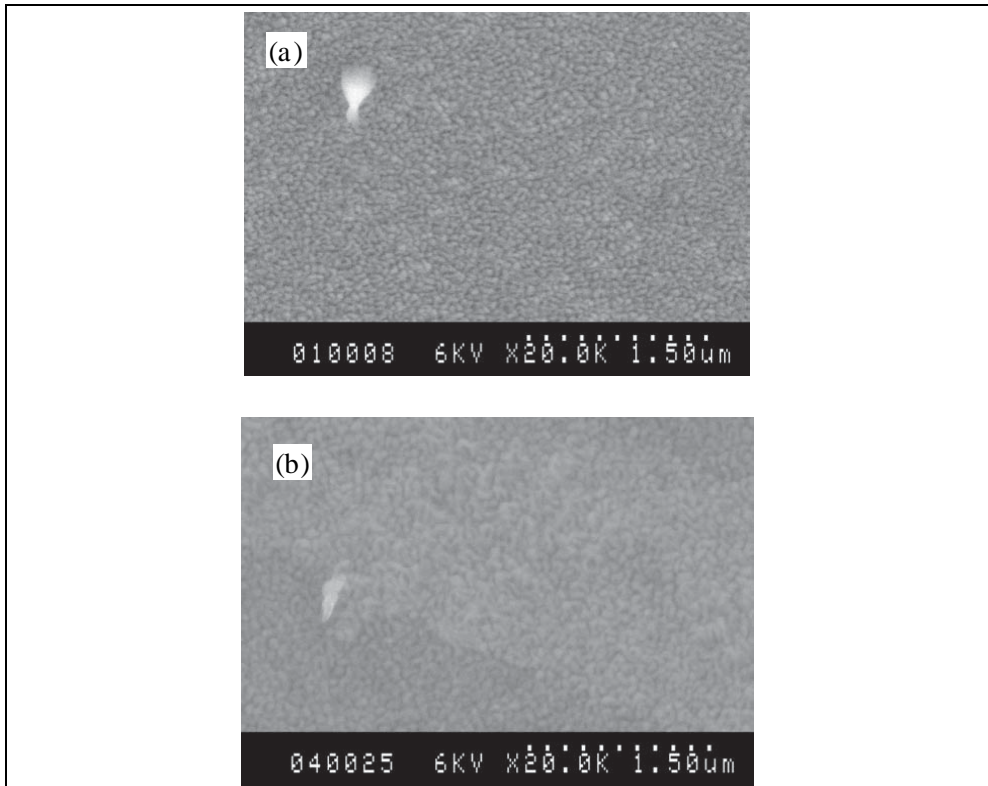


Fig. 3. Scanning electron microscopic image of (a) casting CNTs on the first PP and (b) the completed device.

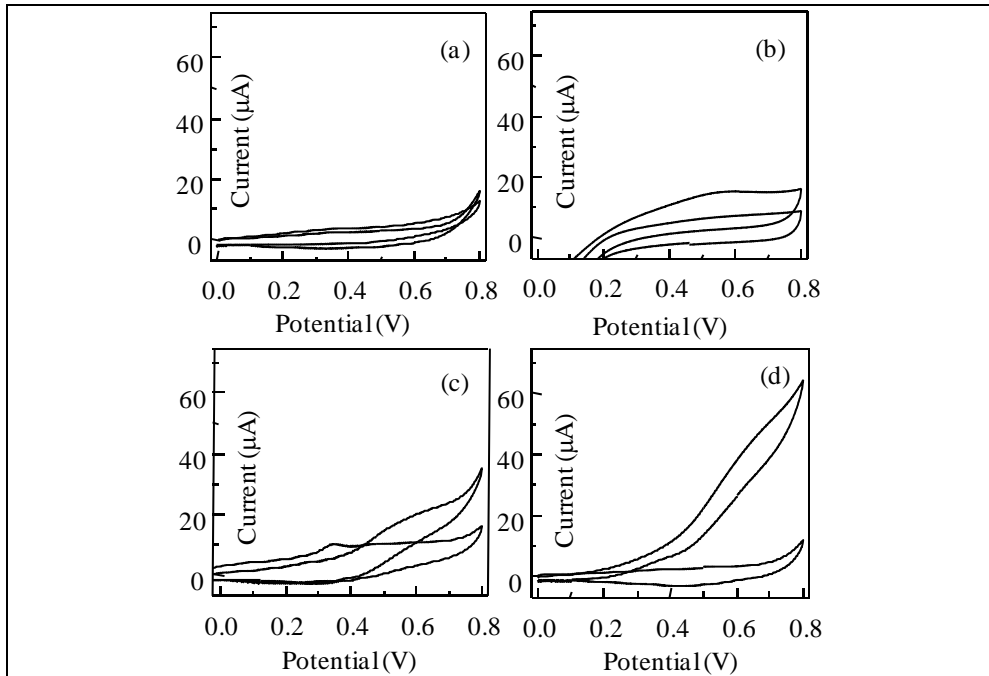


Fig. 4. Glucose response by cyclic voltammetry in the absence and the presence of glucose. The sweep rate was 50 mV s^{-1} , the glucose concentration 48 mM , and the electrolyte used was a pH 7.4, 20 mM phosphate buffer solution. The structures of the devices are (a) PP/GOx/PP/Au (b) PP/GOx/PP/Pt (c) PP/GOx/CNT/Au, and (d) PP/GOx/CNT/PP/Au.

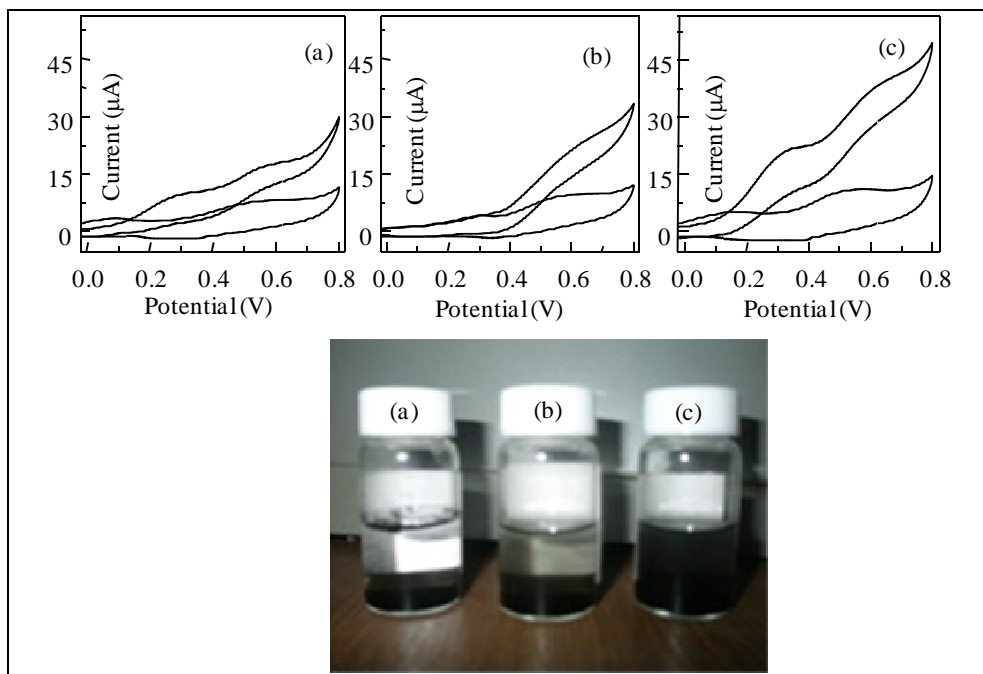


Fig. 5. Cyclic voltammetry of the biosensor response in the presence or absence of glucose. Sweep rate: 50 mV s^{-1} . Glucose concentration: 48 mM ; pH 7.4; 20 mM phosphate buffer solution. Carbon nanotubes were dispersed in (a) buffer solution, (b) ethanol, and (c) 1:1 mixture of buffer solution and ethanol. Photograph: Vials of CNT dispersions after 4 h.

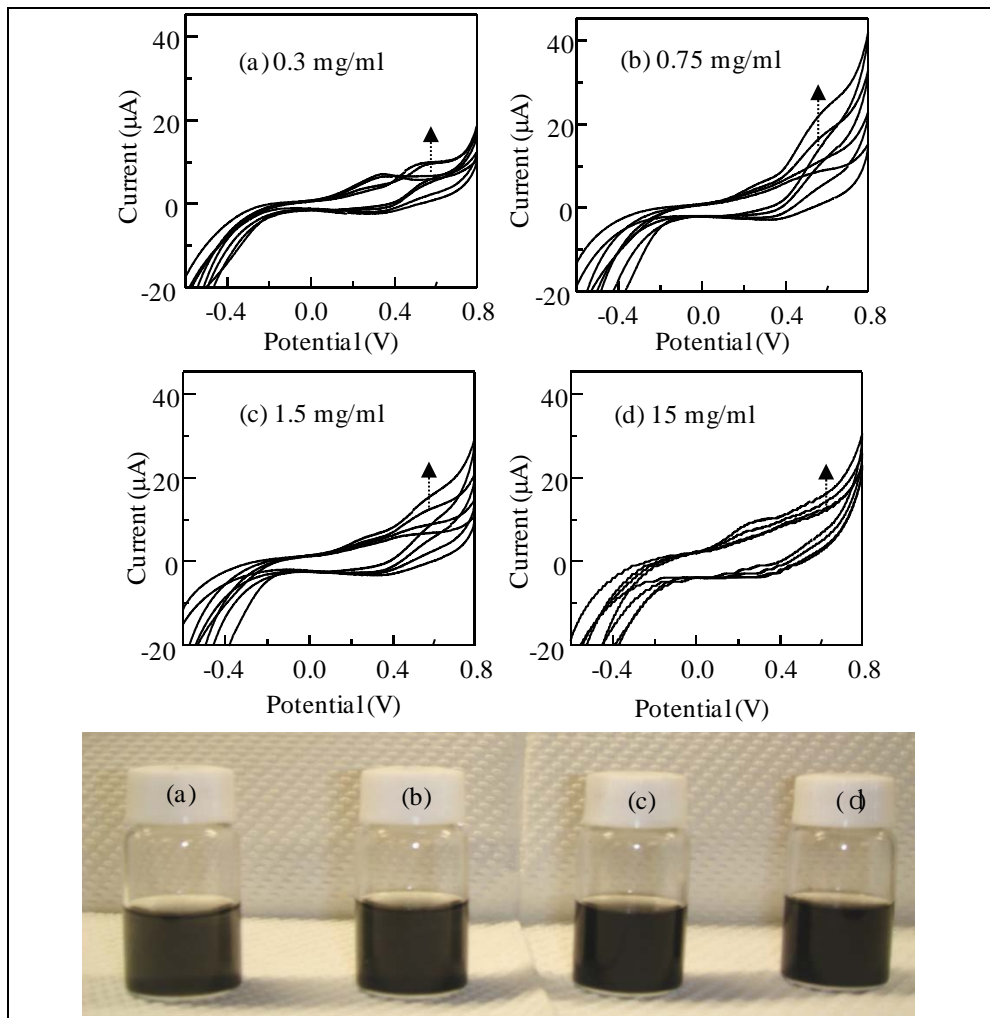


Fig. 6. Cyclic voltammograms of the fabricated amperometric glucose sensor using GOx, CNTs, and PP (PP/GOx/CNT/PP/Au) as a function of the CNT concentration used for casting the CNT layer. CNT concentrations: (a) 0.3, (b) 0.75, (c) 1.5, and (d) 15 mg mL^{-1} . Arrow directions indicate the glucose concentration increments at 0, 2.5, 14, and 48 mM. Conditions: 20 mM phosphate buffer; pH=7.4; 20 °C; scan rate, 50 mV s^{-1} ; electrode area (geometric), 25 mm^2 . Photograph: Vials of CNT dispersions after 4 h.

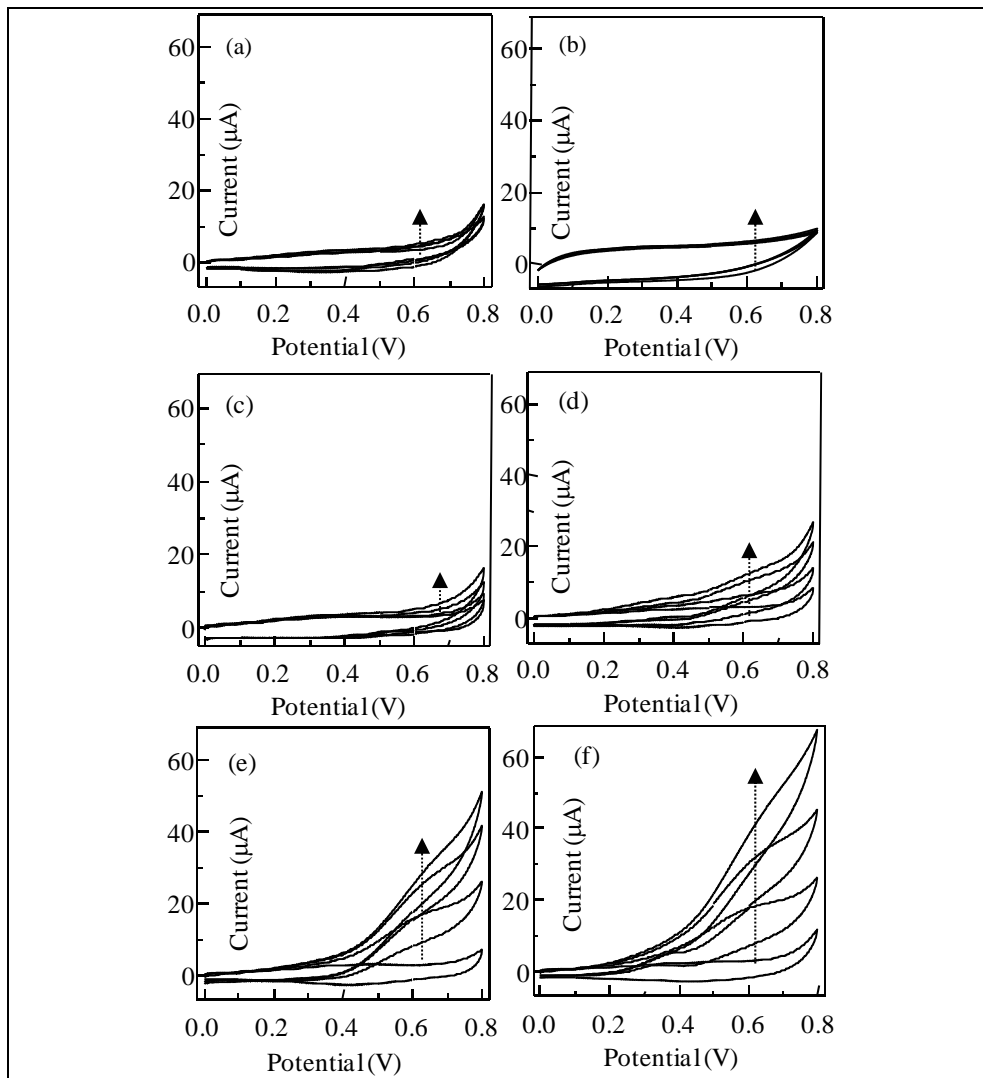


Fig. 7. Cyclic voltammograms of the fabricated amperometric biosensor using SWCNTs and PP in the absence and presence of glucose. Arrow direction represents the glucose concentration increments at 0, 2.5, 14, 35, and 48 mM. Conditions: 20 mM phosphate buffer; pH=7.4; 20 °C; scan rate, 50 mV s⁻¹; electrode geometrical area, 25 mm². (a) PP/GOD/PP/Au. (b) PP/GOD/CNT/PP/Au. (c) PP/GOD/PT-30W/CNT/PP/Au. (d) PP/GOD/PT-50W/CNT/PP/Au. (e) PP/GOD/PT-60W/CNT/PP/Au. (f) PP/GOD/PT-70W/CNT/PP/Au. Title of figure, left justified

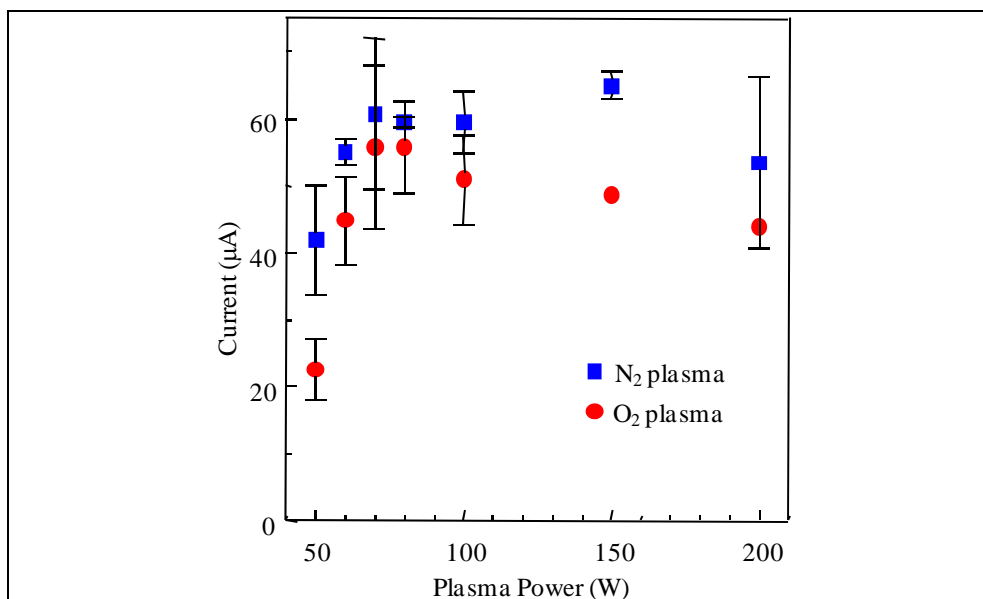


Fig. 8. Dependence of the current response on the plasma power for treatment of the CNT layer on the first PP. Cyclic voltammetry was performed at +0.8 V in the presence of 48 mM glucose, with a sweep rate of 50 mV s⁻¹ in an electrolyte of pH 7.4 20 mM phosphate buffer solution.

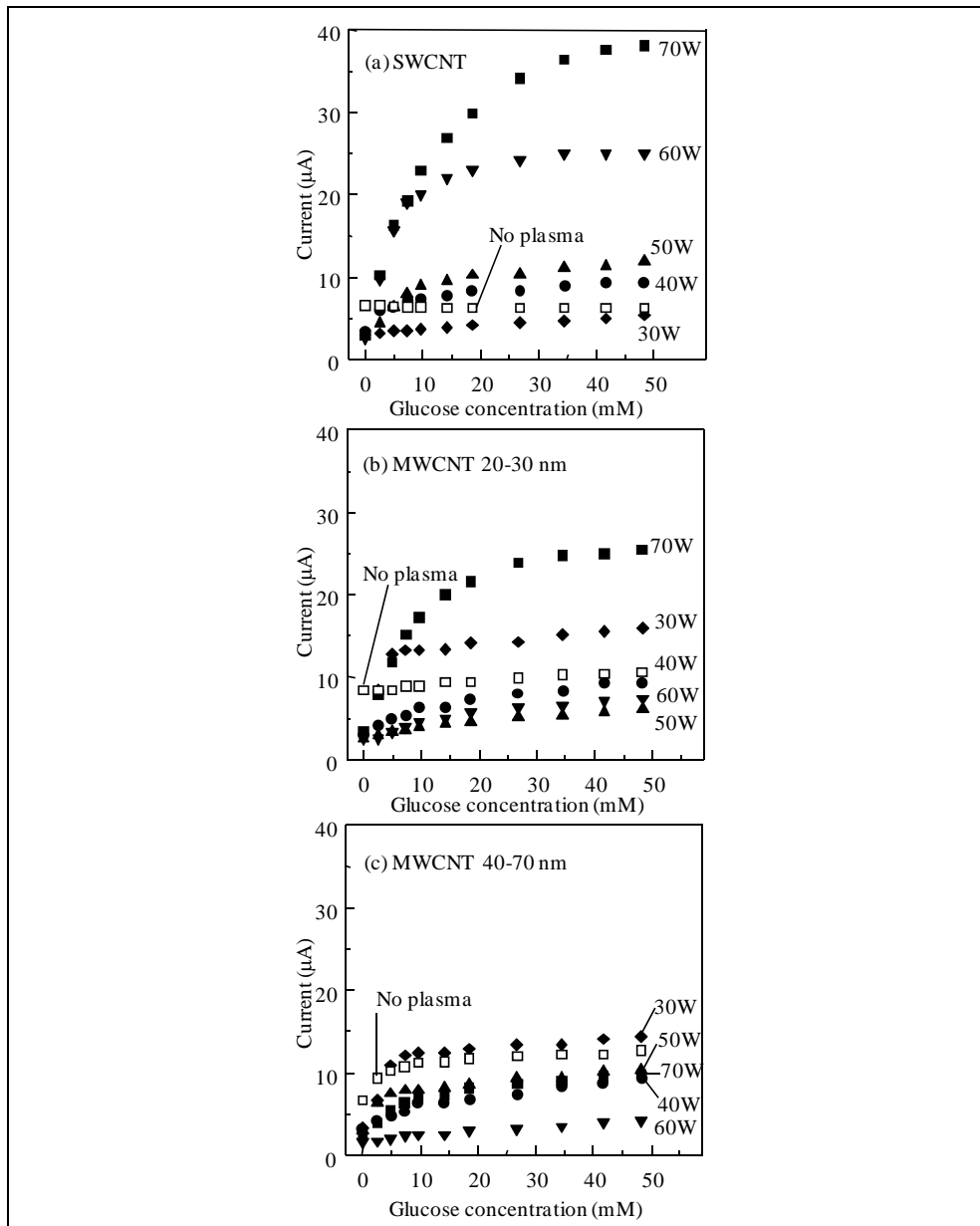


Fig. 9. Calibration of devices in 20 mM phosphate buffer (pH 7.4) with different types of CNTs, (a) SWCNTs, (b) 20-30-nm-diameter MWCNTs, and (c) 40-70-nm-diameter MWCNTs nm as a function of oxygen plasma power for treatment of CNTs: rhombus, 30 W; circle, 40 W; triangle, 50 W; inverse triangle, 60 W; closed square, 70 W; open square, no plasma. The oxidation current at +0.6 V vs. Ag/AgCl under cyclic voltammetry was used.

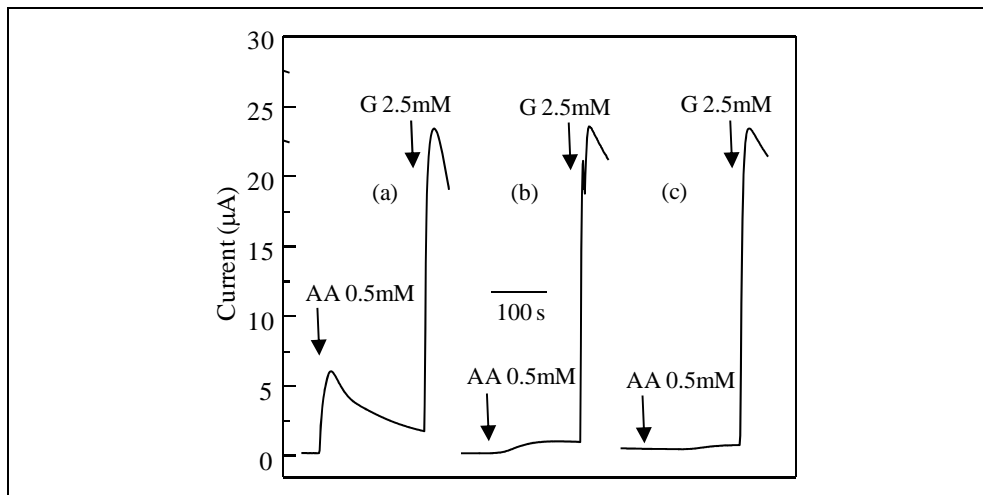


Fig. 10. Amperometric response to 0.5 mM ascorbic acid (AA) and 2.5 mM glucose (G). Acetonitrile plasma polymer coating on the immobilized enzyme: (a) no PP overcoating (GOx/CNT/PP/Au), (b) 10 nm PP overcoat, (10 nm PP/GOx/CNT/PP/Au), and (c) 20 nm PP overcoat (20 nm PP/GOx/CNT/PP/Au). The polarized potential was +0.8 V vs. Ag/AgCl. The electrolyte was a pH 7.4 20 mM phosphate buffer solution.

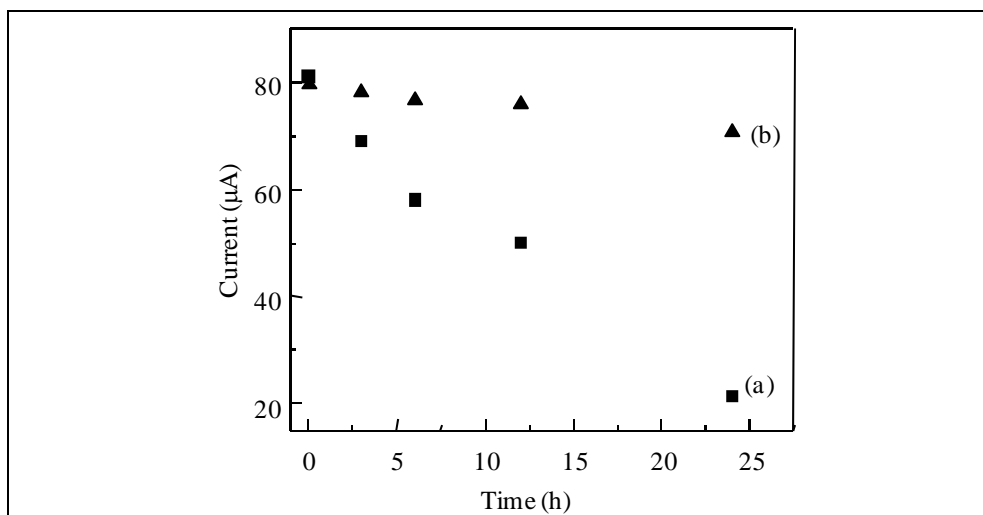


Fig. 11. Operational stability of the biosensor under continuous operation. The polarization potential was +0.8 V vs. Ag/AgCl at a glucose concentration of 48 mM, with an electrolyte of pH 7.4; 20 mM phosphate buffer solution. Working electrodes are (a) GOx/CNT/PP/Au (no overcoating) and (b) PP/GOx/CNT/PP/Au.

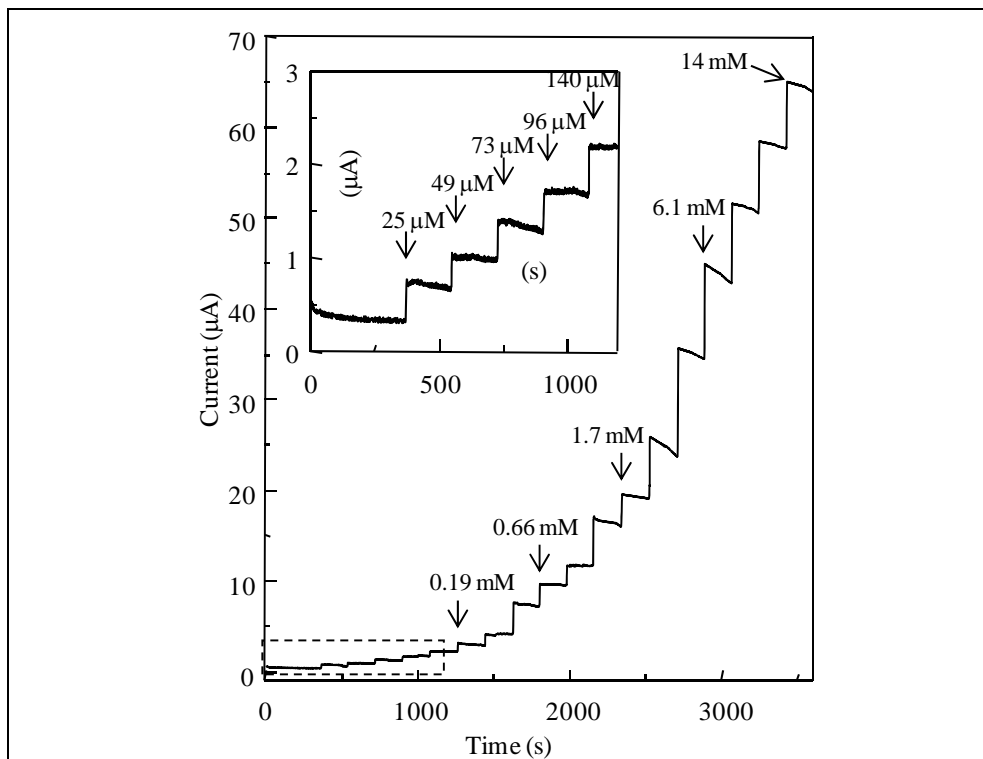


Fig. 12. Time-current response to sequential glucose addition at concentrations of 0.025, 0.049, 0.073, 0.096, 0.14, 0.19, 0.25, 0.45, 0.66, 0.88, 1.3, 1.7, 2.3, 4.2, 6.1, 8.1, 12, and 14 mM. The electrode was 20 nm PP/GOx/CNT/PP/Au, the polarized potential was +0.8 V vs. Ag/AgCl, with an electrolyte of pH 7.4 20 mM phosphate buffer solution. Inset: Enlargement of the region of lower glucose concentration.

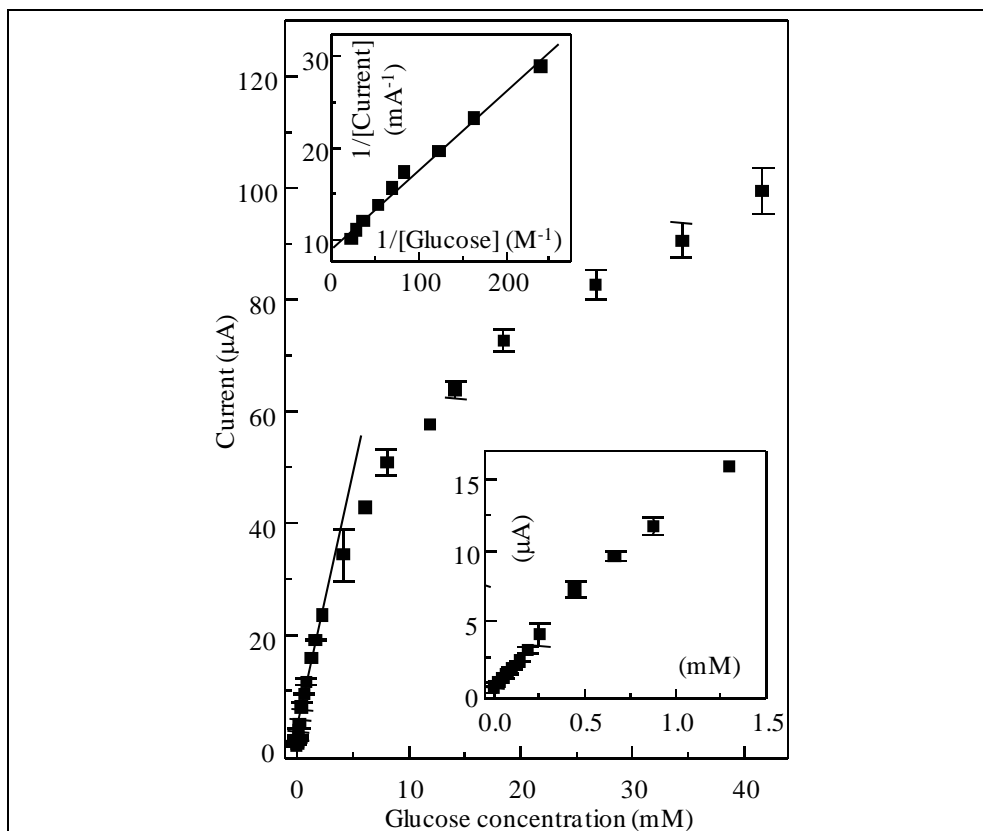


Fig. 13. Calibration plot for glucose response using the data in Fig. 12. Correlation line at low glucose concentration range (0-2.2 mM); sensitivity of 42 mA mM⁻¹ cm⁻² ($r = 0.993$). Lower inset: Enlargement of the low concentration range. Upper inset: Lineweaver-Burk plot. I_{\max} 0.44 mA cm⁻²; K_M^{app} 11 mM.